

Safe Operations of Construction Robots on Human-Robot Collaborative Construction Sites

Marvin H. Cheng¹, Ci-Jyun Liang², and Elena G. Dominguez³

¹Division of Safety Research, National Institute for Occupational Safety and Health, USA

²Department of Civil Engineering, Stony Brook University, USA

³PILZ Automation Safety, USA

MCheng@cdc.gov, Ci-Jyun.Liang@stonybrook.edu

Abstract –

Construction robots have become essential tools on a variety of jobsites. These devices can be revolutionary tools for improving construction efficiency and reducing musculoskeletal disorders and traumatic injuries. However, this innovative technology comes with corresponding dangers and hazards if a robot is not operated properly. Construction workers can be injured by unexpected contact. Therefore, construction robots need to be operated under specific safety procedures to prevent workers from being injured. In this study, a mechanical approach was proposed to derive the dynamic models of unexpected contact during human-robot interaction. With the dynamic models, contact forces and deformations of body parts of human workers can be estimated. The estimated results can be used as reference values to help safety engineers or others to adjust the operations in different scenarios on the construction jobsite for improved safety.

Keywords –

Collaborative Robots; Safety; Mechanical Model

1 Introduction

With the rapid advances in robotics, the construction industry is beginning to be revolutionized with the help of robots designed for this labor-intensive sector [1]. Robotic devices with various functions have been deployed or studied in different applications in the construction sector. With the deployment of various robotic devices, collaborative workspaces that require human-robot interaction have become more common in the past decade. On construction sites, robots are already used to assist construction workers with labor-intensive tasks, such as bricklaying, carrying heavy materials, and demolition tasks [2-3]. Type C mobile robots have been used in construction logistics to prevent long-term musculoskeletal disorders in construction workers [4].

Various research groups have also investigated how robotic on-site additive manufacturing can speed up the construction process [5,6]. Wearable robotic devices have also been widely used to prevent occupational traumatic injuries and musculoskeletal disorders [7]. However, robotic applications deployed on construction sites remain limited due to the lack of computational power, sensory assessment, and effective human-machine interface capabilities, which are important for construction work that requires multiple steps, various tool sets, and the need to follow specific work protocols.

Modern industrial robotic devices can detect the conditions of the jobsite and communicate among each other, sharing site information in real-time. With the capabilities to efficiently sense and communicate between robots, engineers can program robots for upcoming construction jobs to actively assist workers with repetitive tasks while providing required assistance during heavy-duty manual operations. For example, masonry robots have been used to reduce potential injuries due to the need for construction workers to move heavy objects. The collaborative partnership allows construction workers to focus on the quality of the construction tasks as well. However, an open jobsite such as a construction site is often not an ideal environment for robots to have all necessary sensors to detect worker's movements and environmental changes. Environmental disturbance, noises, and an insufficient number of sensors can greatly affect the ability of the robot to detect surrounding hazards and movements of existing objects in the construction space [8]. Thus, although robotic devices can greatly assist construction workers in performing repetitive and labor-intensive tasks and prevent potential injuries, unexpected contact between robots and construction site workers can still be dangerous and even fatal [9,10].

In a human-robot collaborative environment, robots can perform repetitive and labor-intensive work while construction workers focus on planning and inspecting the results to ensure quality. However, human-robot collaboration on construction sites can be dangerous for

a number of reasons, such as the height of the job site, unstructured workspaces, and accidentally dropped items [11]. If safety regulations do not clearly dictate a specific operation, workpieces carried by existing robots could strike human workers while operating in an open environment. In this constrained environment, the robot controllers need to be able to minimize potential injuries from unexpected contact between human workers and a coexisting robotic device, or the payload they carry. Unfortunately, while safety standards for both collaborative and mobile robots have been published for the manufacturing industry, related safety standards for robotic equipment used on collaborative construction sites have not yet been developed. Therefore, the construction industry urgently needs safety guidelines for the use of robotic equipment on open construction sites.

According to recent studies of construction occupational incidents, falling of a person from heights, striking against or struck by moving objects, and struck by falling objects are ranked as the top incident types of occupational injury cases in the construction industry [10]. As an important piece of equipment on the jobsite, many different operational methods have been investigated. In these safety studies, computer vision plays an important role in detecting the presence of construction workers as well as the relative distance between construction workers and robots [12-14]. With the help of computer vision devices, robots can sense the movements of workers around them and identify the contact avoidance zones. The moving trajectory of the robot is then automatically programmed to proactively avoid potential contact with workers in the targeted zone [15]. In addition to path planning methods based on visual feedback, industry and academia have also studied task allocation methods by optimizing the individual capabilities of both robots and human workers [16]. However, most of these human-robot interaction studies focused on applications in manufacturing, healthcare, transportation, and warehouse logistics. Although the developed technologies can be applied to the human-robot collaboration in the construction industry, they are currently not well adopted in construction applications. Some tasks that are not structured enough need to rely on human reasoning in complex manipulation tasks in unstructured environments [17]. The emerging field of human-robot collaboration has significant potential applications in construction and continues to advance the state-of-the-art in defining the roles of both humans and robots in collaborative work. In this study, we focused on a common incident: injury caused by being struck by a moving object. To prevent such an incident, the transferred energy during the impact should not generate a force that yields deformation on a human body surface greater than the permissible values. With this specific condition, the moving speeds of the robot parts, or the

object the robot carries, need to be determined. A mechanical modeling approach was applied to estimate the allowed velocity of the robot at the contact point while the robot is working on its assigned task.

The second section of this manuscript discusses the safety concerns of construction robots. Safety operations of an existing safety standard are assessed whether they are applicable to construction sites. Section three presents the dynamic models for two human-robot collision scenarios. The permissible conditions are discussed in this section. The fourth section discusses the physical conditions for two possible cases of the transient responses of the collision. Proper actions are suggested based on the simulation results in this section. The final section summarizes the overall results of this study.

2 Safety Concerns of Construction Robots

2.1 Safety Standards for Collaborative Robots

Current industrial standards of collaborative robot safety, ANSI/RIA R15.06 [18] and ISO/TS 15066 [19], have identified four types of operations to control injury risks for collaborative robots to work with workers, including safety-rated monitored stop, hand guiding, speed and separation monitoring, and power and force limiting. While these types of operations are effective in protecting workers from potential injury in designated workspaces, some are not as easy to implement on construction sites. For example, a robot that assists carpenters in building a timber frame structure of a residential house needs to team up with the carpenter. In this multi-step task, the robot needs to pass tools, carry materials, slide frames, or hammer components into place [20]. Specific safety operations identified in the safety standards would need to be applied in each step to meet the current safety requirements. Implementing all safety operations can be difficult and time-consuming if the robot needs to complete all the steps of the task. Figure 1 illustrates the interaction between a construction worker and a masonry robot. In this open jobsite, it is difficult to install all the required sensors in the environment for effective safe operation.

2.2 Safety Concerns on Construction Sites

The most effective way to reduce impact injuries from moving robotic devices is to monitor the movements of surrounding construction workers and program the robot's path planning to proactively avoid unexpected contact. Contact between robots and human workers is allowed at designated locations with limited forces. However, while a robot may be able to detect the presence of human workers, it might not be able to continuously monitor the worker's movement from all

directions on an open jobsite. If a robot cannot effectively recognize the worker's movements, it is less likely that the robot can perform all the required safety operations based on the worker's body posture. Thus, there is a need to regulate energy transfer between the human worker and the robot, or the construction material carried by the robot. One important consideration is that the transferred energy caused by unexpected contact should not be greater than a threshold value [21], which shall not cause injury on the surface of different body parts or alter the position of the worker due to the contact.



Figure 1. Human-robot collaboration on the construction jobsite using a masonry robot [22].

Taking these two factors into consideration, several physical criteria need to be defined to program motions of the robot. These two criteria include the permissible deformation of the human body surface and the allowable force in the contact area of the human body. These two values are usually not the same for different human body parts. The allowed deformation of the body surface and the allowed transferred energy can be used to determine moving speed at which the robot moves on contact. In ISO/TS 15066, it is recommended that the end-effector of a robotic device should move less than 0.25 m/s when the presence of a human worker is detected [19].

3 Modeling of Impacts Between Human Workers and Robotic Devices

To develop safety requirements on collaborative construction sites, knowledge of the environment and operation of construction robots is required. The construction site is usually an open environment, so the number of sensors can be limited and not easy to install. Although the parameters of the robot, such as the moving speed of the end effector, the angular positions and velocities of joints, and the effective configuration space, can be obtained from the controller of the robot, information related to the moving speeds of surrounding workers and changes of geometric shapes of the worksite may not be readily available. Without these data being readily acquired, robotic devices need to determine

operations based only on the detectable characteristics, such as moving speeds and locations. Thus, operations need to be adjusted if the presence of human workers is detected. In this section, two contact models were investigated to determine the physical interaction of the unexpected contact between human workers and robotic devices. In this study, two cases of unexpected contact were considered:

1. Struck and pushed: The robot contacts the worker and forcibly moves the worker from his/her original position.
2. Struck and bent: The robot contacts the worker from behind, and the worker's upper body bends forward around the waist joint. The lower body of the worker remains unmoved.

To derive the dynamic models of these impact scenarios, the equations of motion of the whole body need to be derived. However, each model needs to be divided into two phases. The first phase is the compression phase, starting from the contact between the object and the human body surface, until the compression reaches the permissible deformation of the human body. The second phase is the retraction phase, where the body surface begins to recover from its permissible deformation to its original state. The contact area of the body part acts in the first phase as a mass-damper-spring system. During the retraction phase, the elastic force exists only when the interaction force between the body surface and the object is greater than zero. Once the interaction force disappears, or the object is no longer in contact with the human body, the moving object is excluded from this mass-damper-spring system, but the skin surface is still deformed due to the previous impact. The configuration of the compression and retraction phases is shown as Figure 2.

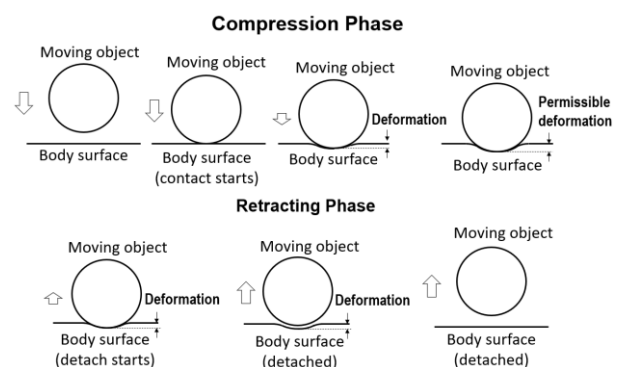


Figure 2. Compression and retraction of reaction of between skin surface and moving object due to impact.

3.1 Struck and Pushed

For the impact between a moving object and a human worker, Figure 3 demonstrates the mechanical model of such an impact. Depending on the initial velocity of the moving object carried by the robot, the dynamic response is also different. If the initial speed of the robot is below a threshold, the object bounces back after impact. If the initial velocity of the object transported by the robot is too fast, the contact surface of the worker's body is compressed to the maximum, and the worker's body moves together with the object. In this case, the object and the worker move with the same final velocity. If the object carried by the robot is heavy and moving too fast, the worker can be thrown out after being impacted. The last two situations can lead to severe worker injury and should be avoided when human workers collaborate with robotic devices in the workspace. In this study, only the first situation is discussed. Figure 3 illustrates the situation when an object carried by the robot strikes the worker from the side. In this configuration, the horizontal movement of the object transported by the robot is x_B , and the horizontal movement of the center of mass of the worker's body is x_h . The equations of motion of the worker and the moving object can be written as

$$M_B \ddot{x}_B + C_h \dot{x}_B - C_h \dot{x}_h + K_h x_B - K_h x_h = 0 \quad (1)$$

$$M_h \ddot{x}_h + C_h \dot{x}_h - C_h \dot{x}_B + K_h x_h - K_h x_B - K_h x_B + f_s = 0 \quad (2)$$

where the mass of the moving object is M_B , the mass of the human body is M_h , the stiffness of the contact surface of the body part is K_h , the corresponding viscous damping is C_h , and f_s is the static friction between the shoes and the ground. The compression of the body at the impact location Δs is

$$\Delta s = x_B - x_h \quad (3)$$

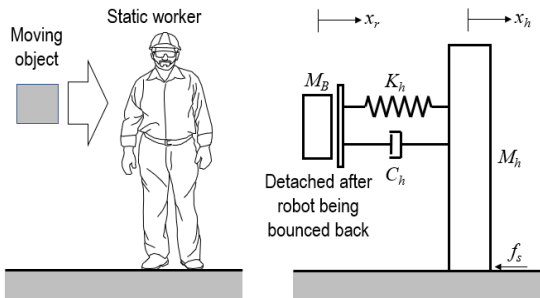


Figure 3. Mechanical model of the side impact between the static worker and the moving robot.

The contact force F_c that yields the compression on the human body is

$$F_c = K_h \Delta s_{max} \quad (4)$$

The contact force reaches its maximum when the

deformation Δs is also its maximum. The initial velocity of the moving object at the moment of contact is \dot{x}_{B0} . In the compression phase, the object carried by the robot compresses the human body surface until the relative velocity is zero. Then the retraction phase starts. Once the object is detached from the worker's body, or the surface of the worker is no longer compressed, the object stops interacting with the worker's body. Therefore, the worker is no longer subjected to the external force from the object. The velocities of the worker and the object after the impact can also be verified by conservation of momentum, which is

$$M_B \dot{x}_{B0} + M_h \dot{x}_{h0} = M_B \dot{x}_B(t) + M_h \dot{x}_h(t) \quad (5)$$

In this configuration, three possible outcomes are expected. If the moving speed of the object is low, the body surface of the worker might deform without moving the entire body. In this case, the static friction between the worker and the floor is high enough to prevent the worker from moving. The worker can also move after the impact. In this case, the object might bounce off of the worker after impact, and the friction between the worker and the floor changes from static to kinetic friction. If the object is moving fast enough, the object might push the worker and move the worker with it. Then the friction changes from static friction to kinetic friction.

3.2 Struck and Bent

To derive the dynamic model of the two phases, Figure 4 demonstrates the mechanical model of the impact. In this configuration, the horizontal movement of the moving object driven by the robot is x_B , and the angular movement of the upper body, or the waist joint, is θ_u . It is assumed the object contacts the human worker's back. An assumption has been made that the upper body center of mass is at one-half the upper body length. The horizontal movement of the center of mass of the work's upper body is x_h , which is

$$x_h = \frac{l_u}{2} \theta_u \quad (6)$$

The corresponding moving velocities and accelerations of the object carried by the robot and the affected worker are \dot{x}_B , \dot{x}_h , \ddot{x}_B , and \ddot{x}_h , individually. The range of motion of the waist joint is limited according to the physical condition of the worker, which is $\theta_{u,max}$. In the compression phase, the initial contact velocity of the moving object is \dot{x}_{B0} . When contact starts, the moving velocity and the angular velocity of the upper body of the worker are $\dot{x}_{h0} = 0$ and $\dot{\theta}_{u0} = 0$. The mass of the upper body is M_{hu} , and the length of the upper body is l_u . The lower body, including the thighs, legs, and feet are lumped as a single mass $M_{l,lumped}$. The compression of the body at the impact location Δs is $x_B - x_h$, which is

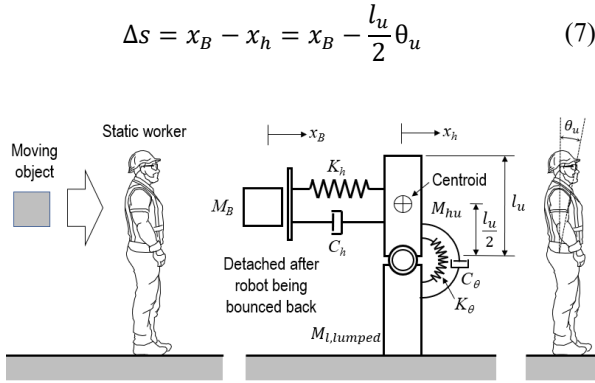


Figure 4. Mechanical model of the back impact between the static worker and the moving robot.

With this configuration, the equations of motion of both the moving object and worker's upper body in the first phase can be described as

$$M_B \ddot{x}_B + C_h \dot{x}_B - \frac{C_h l_u}{2} \dot{\theta}_u + K_h x_B - \frac{k_\theta l_u}{2} \theta_u = 0 \quad (8)$$

and

$$\frac{M_{hu} l_u^2}{4} \ddot{\theta}_u - \frac{C_h l_u}{2} \dot{x}_B + \left(C_\theta + \frac{C_h l_u^2}{4} \right) \dot{\theta}_u - \frac{k_\theta l_u}{2} x_B + \left(\frac{K_h l_u^2}{4} + k_\theta \right) \theta_u = 0 \quad (9)$$

where M_{hu} is the mass of the upper body, and k_θ is the stiffness of the joint between the upper and the lower body. During the whole impact process, there is no external force applied to either the robotic device or the worker. The maximal force occurs during the approaching process before the compression Δs reaches to its maximum. The contact force F_c that yields compression on the human body is

$$F_c = K_h \Delta s_{max} \quad (10)$$

The contact force reaches to its maximum when the deformation Δs is also maximum. Then the process of impact changes to the retraction phase. Once the moving object separates from the worker's body, the object stops interacting with the worker's body. The detachment occurs in the retraction phase. Though the body surface has not returned to its original position, the moving object has moved a sufficient distance and no longer touches the body surface of the worker. After the robot is separated from the worker, it moves at a constant speed. Since the interaction between the human body and the object carried by the robot no longer exists, the contact force generated by the impact also becomes zero. The human postures still change due to the dynamics induced by the stiffness and viscous properties of the human body. Thus, the equation of motion of the worker's body becomes

$$\frac{M_{hu} l_u^2}{4} \ddot{\theta}_u + C_\theta \dot{\theta}_u + k_\theta \theta_u = 0 \quad (10)$$

By modeling the dynamics of the given status, the maximum compression of the body surface and the related contact force can be derived if the initial velocity of the moving object is given. If the permissible compression on the human body is specified, an upper limit for the contact velocity of the object can also be established. Additionally, the worker cannot maintain a stationary location if the worker's center of gravity is not within the area of support, or the feet.

3.3 Allowed Pressure and Permissible Deformation at Different Body Parts

To prevent potential injuries from robot operations, unexpected contact between object carried by robot and human workers needs to be avoided. However, if the potential contact is likely to occur at a collaborative worksite, the speed at which the robot moves needs to be regulated to prevent injury. To determine the permissible moving speed of the robotic device while transporting construction materials, two parameters are required, permissible impact force and permissible deformation. In ISO/TS 15066 [19], maximum impact force and stiffness for different body parts are specified. Table 1 lists the values of these properties. The permissible deformation of individual parts can be calculated from the maximum permissible impact force and the corresponding stiffness. In ISO/TS 15066, the permissible pressure multiplier in a transient process is 2, which means the deformation can be doubled during the impact.

Table 1. Stiffness, allowable impact forces, and surface pressure regulated in ISO/TS 15066 [19].

Body part	Impact force (N)	Surface pressure (N/mm ²)	Stiffness (N/mm)
Skull/forehead	175	0.3	150
Face	90	0.2	75
Neck (sides/neck)	190	0.5	50
Neck (front/larynx)	35	0.1	--
Back/shoulders	250	0.7	35
Chest	210	0.45	25
Belly	160	0.35	10
Pelvis	250	0.75	25
Buttocks	250	0.8	--
Upper arm/elbow	190	0.5	30
Lower arm/hand	220	0.5	40
Hand/finger	180	0.6	75
Thigh/knee	250	0.8	50
Lower leg	170	0.45	60
Feet/toes/joint	160	0.45	--

4 Physical Conditions and Simulation Results

To estimate the speed limit of a robot for transporting construction materials on a worksite, a collaborative masonry robot was used to simulate the collision between a standard cored concrete masonry block and a construction worker. In this simulated scenario, a masonry robot assists construction workers in moving concrete blocks for bricklaying.

4.1 Physical Parameters of Human Body and Robotic Device

To estimate the upper limit of the moving speed of the construction materials carried by the robot, the physical conditions of the human worker and the robot need to be specified in the simulation. In the case of struck and pushed, it is assumed that the block touches the upper arm of the worker. In the case of struck and bent, the block contacts the worker's back. In both cases, two types of concrete masonry units (CMUs) were used in the simulation. The dimensions of these blocks were 203.2 mm × 203.2 mm × 406.4 mm (~17 kg) and 203.2 mm × 304.8 mm × 406.4 mm (~25 kg), individually. The worker's height and weight were assumed to be 1.75 m and 90.71 kg, respectively, based on the record of average height and weight of adult males in the United States [23]. According to [25], the upper body includes 55.1% of the total male body mass [24]. The stiffness and the viscous damping of the back surface used in the simulation were 35 N/mm [19] and 100 Ns/mm [25]. The stiffness of the surface on the human's upper arm is 30 N/mm. The stiffness and viscous damping of the waist joint used in the simulation were 366 Nm/rad [26] and 60 Nm/rad [27], individually. Viscous damping has only been partially validated. This value may vary for various reasons, such as age, fatigue level, and physical condition.

According to ISO/TS 15066 (see Table 1), the constant force applied to the back of the human body should not be greater than 250 N. The multiplier of the maximum permissible force during the transient contact is 2, that is, the maximum force of impact should be less than 500 N. Assuming that the deformation of the body surface is within the linear range, the permissible deformation is defined as

$$\text{Permissible deformation} = 2 \times \frac{\text{Allowable force}}{\text{Stiffness}} \quad (10)$$

According to this value, the permissible deformation is 14.3 mm if an unexpected contact does occur on the worker's back at the construction site. The constant force applied to the upper arm of the human body should not be greater than 190 N. The multiplier of the maximum permissible force during the transient contact is 2. This means the maximum impact force should be less than 380

N. Correspondingly, the permissible deformation is 12.7 mm if an unexpected contact does occur on the worker's upper arm. In the case of struck and pushed, the human worker might be moved by the impact. Whether the human worker can be moved depends on the friction between the shoes and the floor, which depends on the level of the striking force. The coefficient of static friction between a rubber shoe sole and dry ceramic floor is between 0.8 to 1.2. On wet floors, this value changes to ~0.3 [28]. In this study, 0.9 was used as the static friction coefficient.

4.2 Simulated Results of Struck and Pushed

In the case of struck and pushed, the 17 kg and 25 kg CMUs collided with the human worker from the upper arm on the side of the worker's body. Figure 5 and Figure 6 demonstrate the transient responses of the two individual impacts. The interactions shown in the figures started from the initial contact between the moving object and the human worker, to the time the object detached from the human body. The worker was not moved until the contact force was greater than the static friction force. Once the worker was moved by the CMU block, the contact force existed until the block was separated from the worker. With the permissible deformation being specified as 12.7 mm, the maximum velocities of 17 kg and 25 kg blocks are 760 mm/s and 680 mm/s. The contact forces in both scenarios are around 380 N, and the worker was moved away from the original location.

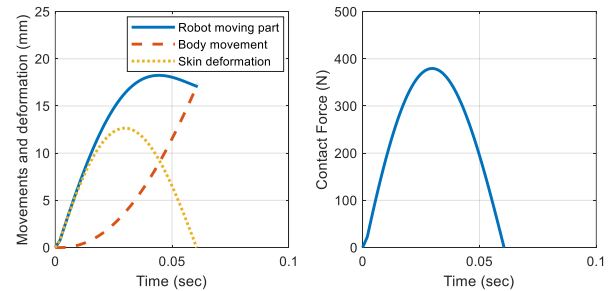


Figure 5. Struck and pushed between the worker and the CMU (17 kg) with 760 mm/s at contact.

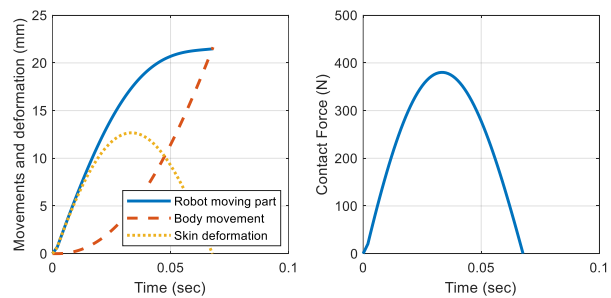


Figure 6. Struck and pushed between the worker and the CMU (25 kg) with 680 mm/s at contact.

4.3 Simulated Results of Struck and Bent

In this case, the 17 kg and 25 kg CMUs collided with the worker from behind on the worker's back. Figure 7 and Figure 8 demonstrate the transient responses of these collisions. With ~ 14 mm of the permissible deformation on the back, the maximum allowed contact velocity is 700 mm/s for a 17 kg block and 570 mm/s for a 25 kg block. In both cases, the maximum interaction force was around 490 N. In this simulation, it was assumed that the worker's foot remains at the same location without moving. All of the energy was absorbed by the viscous damping and bending of the worker's upper body.

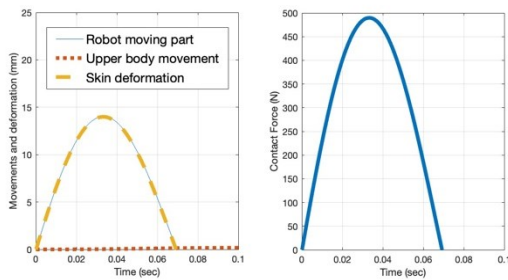


Figure 7. Struck and bent between the worker back and the CMU (17 kg) with 700 m/s at contact.

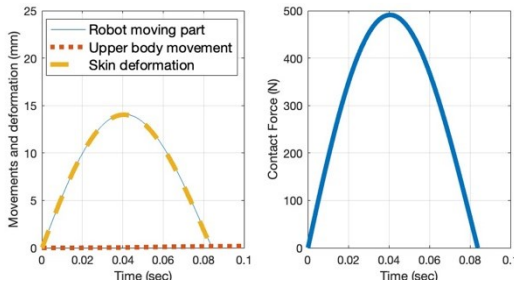


Figure 8. Struck and bent between the worker back and the CMU (25 kg) with 570 m/s at contact.

4.4 Suggested Operation

From the simulation results, the contact forces applied on the body surface and the corresponding deformation can be derived from the contact velocity \dot{x}_B . As the contact velocity increases, the chance of deformation and potential injuries both increases. The proposed model can be used to estimate the operating speeds of robotic devices while transporting materials and collaborating with construction workers on site. In this simulated environment, a male worker was working on a dry construction site. According to the simulated results, the case of struck and bent requires the payload of the robot to move at slower speeds to avoid greater contact force than the case of struck and pushed. Thus, the maximum speed of the masonry robot should be less than 700 mm/s if the robot is carrying a 17 kg block. The

maximum speed is 570 mm/s if the robot is carrying a 25 kg block. When the robot operates at the recommended speeds, it can ensure that the body surface deformation is less than the permissible value if collision does occur. Potential injury from unexpected contact or collision can thus be adequately prevented.

Table 2. Calculated deformations on body surface and contact forces applied on human body.

M_B	Struct and Bent (Back)				Struck and Pushed (Upper Arm)			
	17 kg		25 kg		17 kg		25 kg	
\dot{x}_B	Δs	F_c	Δs	F_c	Δs	F_c	Δs	F_c
200	4	140	4.9	172	2.2	65	2.3	70
300	6	210	7.4	258	3.9	117	4.3	128
400	8	280	9.8	345	5.7	172	6.4	192
500	10	350	12.3	431	7.6	229	8.6	258
600	12	420	14.8	517	9.5	286	10.9	326
700	14	490	17.2	603	11.5	344	13.1	394
800	16	560	19.7	689	13.4	403	15.4	463
900	18	630	22.1	775	15.4	462	17.7	532
1000	20	700	24.6	861	17.4	521	20.1	602

\dot{x}_B (mm/s), Δs (mm), F_c (N)

5 Conclusion

This study presents a simulation approach based on equations of motion to analyze the deformation of the human body during impact while using a construction collaborative robotic device. Appropriate operating speeds can be estimated based on the proposed dynamic models of human-robot interaction. This approach can provide reference values for safely operating robots on construction sites. In the future, dynamic models for different scenarios and different operational environments could be developed, such as rainy weather and muddy ground.

References

- [1] Pan M. and Pan W. Stakeholder perceptions of the future application of construction robots for buildings in a dialectical system framework. *Journal of Management in Engineering*, 36(6): 04020080, 2020.
- [2] Melenbrink N., Werfel J., and Menges A. On-site autonomous construction robots: Towards unsupervised building. *Automation in construction*, 119: 103312, 2020.
- [3] Liang C. J., Wang X., Kamat V. R., and Menassa C. C. Human-robot collaboration in construction: classification and research trends. *Journal of Construction Engineering and Management*, 147(10): 03121006, 2021.

- [4] Follini C., Terzer M., Marcher C., Giusti A., and Matt D. T. Combining the robot operating system with building information modeling for robotic applications in construction logistics. In *Proceedings of the International Conference on Robotics in Alpe-Adria-Danube Region (RAAD)*, page 245-253, Kaiserslautern, Germany, 2020.
- [5] Lim S., Buswell R. A., Le T. T., Austin S. A., Gibb A. G., and Thorpe T. Developments in construction-scale additive manufacturing processes. *Automation in construction*, 21: 262-268, 2012.
- [6] Paolini A., Kollmannsberger S., and Rank E. Additive manufacturing in construction: A review on processes, applications, and digital planning methods. *Additive manufacturing*, 30: 100894, 2019.
- [7] Cho Y.K., Kim K., Ma S., and Ueda J. A robotic wearable exoskeleton for construction worker's safety and health. In *Proceedings of Construction Research Congress (CRC)*, page 19-28, New Orleans, LA, 2018.
- [8] Liang C. J., Lundeen K. M., McGee W., Menassa C. C., Lee S. H., and Kamat V. R. A vision-based marker-less pose estimation system for articulated construction robots. *Automation in Construction*, 104: 80-94, 2019
- [9] Liang C. J., Kamat V. R., and Menassa C. C. Teaching robots to perform quasi-repetitive construction tasks through human demonstration. *Automation in Construction*, 120: 103370, 2020.
- [10] Shafique M. and Rafiq M. An overview of construction occupational accidents in Hong Kong: A recent trend and future perspectives. *Applied Sciences*, 9(10): 2069, 2019.
- [11] Liang C. J. and Cheng M. H. Trends in robotics research in occupational safety and health: a scientometric analysis and review. *International Journal of Environmental Research and Public Health*, 20(10): 5904, 2023.
- [12] Liu H. and Wang L. Gesture recognition for human-robot collaboration: A review. *International Journal of Industrial Ergonomics*, 68: 355-367, 2018.
- [13] Ragaglia M., Zanchettin A. M., and Rocco P. Trajectory generation algorithm for safe human-robot collaboration based on multiple depth sensor measurements. *Mechatronics*, 55: 267-281, 2018.
- [14] Scimmi L.S., Melchiorre M., Troise M., Mauro S., and Pastorelli S. A practical and effective layout for a safe human-robot collaborative assembly task. *Applied Sciences*, 11(4): 1763, 2021.
- [15] Cheng M. H. Real-time adjustment of moving trajectories for collaborative robotic devices. presented at *the 2022 National Occupational Injury Research Symposium*, Morgantown, WV.
- [16] Müller R., Vette M., and Geenen A. Skill-based dynamic task allocation in human-robot-cooperation with the example of welding application. *Procedia Manufacturing*, 11: 13-21, 2017.
- [17] Brosque C., Galbally E., Khatib O., and Fischer M. Human-robot collaboration in construction: Opportunities and challenges. In *Proceedings of the International Congress on Human-Computer Interaction, Optimization and Robotic Applications (HORA)*, pages 1-8, Ankara, Turkey, 2020.
- [18] American National Standard for industrial robots and robot systems – Safety requirements, ANSI Standard R15.06, 2012.
- [19] Robots and robotic devices – Collaborative robots, ISO Technical Specification 15066, 2016.
- [20] Reinhardt D., Haeusler M. H., London K., Loke L., Feng Y., de Oliveira Barata E., Firth C., Dunn K., Khean N., Fabbri A., Wozniak-O'Connor D., and Masuda R. CoBuilt 4.0: Investigating the potential of collaborative robotics for subject matter experts. *International Journal of Architectural Computing*, 18(4): 353-370, 2020.
- [21] Unfallversicherung D.G. *BG/BGIA Risk Assessment Recommendations According to Machinery Directive: Design of Workplaces with Collaborative Robots*, Institute for Occupational Safety and Health of the German Social Accident Insurance, Sankt Augustin, Germany, 2009.
- [22] Lampus, Mule Lifting Systems by Construction Robotics. Online: <https://www.lampus.com/Product-MULE-Lifting-System>, Accessed: 31/10/2023.
- [23] Fryar C. D., Carroll M. D., Gu Q., Afful J., and Ogden C. L. Anthropometric reference data for children and adults: United States, 2015–2018. *National Center for Health Statistics, State 3*, 46, Washington, D.C., 2021.
- [24] Plagenhoef S., Evans F. G., and Abdelnour T. Anatomical data for analyzing human motion. *Research Quarterly for Exercise and Sport*, 54: 169-178, 1983.
- [25] de Leva P. Adjustments to Zatsiorsky-Seluyanov's Segment Inertia Parameters. *Journal of Biomechanics*, 29(9): 1223-1230, 1996.
- [26] Farley C. T. and Morgenroth D. C. Leg stiffness primarily depends on ankle stiffness during human hopping. *Journal of Biomechanics*, 32: 267-273, 1999.
- [27] Desplantez A., Cornu C., and Goubel F. Viscous properties of human muscle during contraction. *Journal of Biomechanics*, 32: 555-562, 1999.
- [28] Mohamed M. K., Samy A. M., and Ali W. Y. Friction Coefficient of Rubber Shoe Soles Sliding Against Ceramic Flooring. *KGK*, 64(4): 44-49, 2011.